

Submitted to *INFORMS Journal on Optimization*  
manuscript (Please, provide the manuscript number!)

Authors are encouraged to submit new papers to INFORMS journals by means of a style file template, which includes the journal title. However, use of a template does not certify that the paper has been accepted for publication in the named journal. INFORMS journal templates are for the exclusive purpose of submitting to an INFORMS journal and should not be used to distribute the papers in print or online or to submit the papers to another publication.

# Novel Target Discovery of Existing Therapies: Path to Personalized Cancer Therapy

Dimitris Bertsimas

Sloan School of Management and Operations Research Center, Massachusetts Institute of Technology, Cambridge, MA 02139,  
dbertsim@mit.edu

Ying Daisy Zhuo

Sloan School of Management and Operations Research Center, Massachusetts Institute of Technology, Cambridge, MA 02139,  
zhuo@mit.edu

Discovering new drugs involves tremendous effort and financial resources, often at a significant risk of failed trials. Identifying new targets of existing drugs provides a promising direction, especially for molecular targeted cancer therapies. This paper presents a novel, machine learning and optimization-based method that identifies potential targets of existing drugs to expand the treatable patient population. The method has the following advantages: 1) it is based on clinical and genomic data from a large national cancer hospital; 2) it incorporates state-of-the-art knowledge of cancer molecular biology and signaling pathways; 3) it models patient heterogeneity explicitly outside genomics. The output is an ordered list of therapy-target pairs that our algorithm identifies as highly promising to be further tested. The results are highly accurate when validated against known mechanisms of action for existing drugs, where relationships such as pertuzumab-ERBB2, cetuximab-EGFR, and erlotinib-EGFR were independently identified. We found similar results in the external The Cancer Genome Atlas data set. The findings suggest that a data-driven optimization approach to precision cancer medicine may lead to breakthroughs in the drug discovery process and recommend effective personalized cancer treatments given patient-specific genomic and phenotypic information.

*Key words:* mixed integer optimization, targeted therapy, cancer genomics

---

## 1. Introduction

Drug discovery is a costly and slow process. The average cost of developing a new pharmaceutical drug has risen to 2.5 billion in the United States (DiMasi et al. 2016), and the average time from discovery to market is estimated to be 13.5 years (Paul et al. 2010). The high cost does not necessarily translate to the clinical efficacy of drug candidates identified; in fact, only 11% of drugs in clinical trials are eventually approved.

This increasing burden, risk, and low return-on-investment from *de novo* drug discovery have forced drug developers to look at alternatives. Repurposing existing drugs for novel uses is an attractive option to improve the research and development productivity, so long as the drugs turn out to be clinically effective on the novel uses identified. As the toxicity profile and pharmacokinetics of existing drugs has been extensively tested in prior trials, effective drug repurposing can significantly reduce the cost and regulatory approval time frame.

Cancer therapeutic development presents a particular opportunity for alternatives to *de novo* drug discovery. The advances in understanding of cancer biology at the molecular level and the wide availability of genetic biomarker testing expanded cancer drugs from traditional cytotoxic chemotherapies to more focused targeted therapies in the past decade (Hanahan and Weinberg 2011). These drugs interfere with specific molecular targets that are involved in the growth, progression, and spread of cancer, and have demonstrated promising efficacy and tolerability for cancer patients in clinical settings.

Yet as cancer therapies are becoming more precision-based and individualized, the size of patient cohorts with the specific molecular biomarker for a new drug continues to decline. In 2016, more than 40% of newly approved drugs have the orphan designation (indicated for fewer than 200,000 Americans), among which half are cancer drugs (U.S. Food and Drug Administration 2016). Between 2009 and 2015, FDA approved 12 orphan cancer drugs indicated for biomarker-defined subsets (Kesselheim et al. 2017). If additional targets are identified for these highly specialized drugs, the increased market size can justify the high research and development cost.

Drug repurposing in cancer has seen some success stories. A notable example is crizotinib, first developed for anaplastic large-cell lymphoma as a MET inhibitor. Its ALK inhibiting properties was later discovered and therefore repositioned to treat a subpopulation of non-small cell lung cancer (NSCLC). The approval process for NSCLC took only 4 years, significantly shorter than the average time (Shaw et al. 2011, Li and Jones 2012). Imatinib, originally approved in 2001 for chronic myelogenous leukemia (CML), now has many indications including for patients with KIT positive gastrointestinal stromal tumors (GIST) (Novartis 2017, Druker 2004). Many such hidden interactions remain to be discovered; it is estimated from known databases that on average a targeted cancer drug interacts with six molecular targets (Mestres et al. 2009).

Identifying such novel drug-target relationship accurately is, unfortunately, a difficult problem. The current approach to find new targets of existing drugs in practice typically relies on pure serendipity or anecdotal evidence. The combinatorial nature of the drug-target network prohibits the conventional trial-and-error process to be effective, as the number of possibilities explodes with respect to number of potential targets. With next-generation genome sequencing becoming more widely available, additional potential targets are identified, creating further opportunities as well as challenges for drug repurposing.

As a result, systematic, statistical, and computational approaches are needed for such discovery. In the past decade, progress has been made leveraging various data sources to suggest new targets and drug indications (Chen and Butte 2016, Li et al. 2015). In one strategy, the relationship is inferred based on the structural and chemical similarity between drugs (Li and Lu 2012), and/or based on existing indications and documented side effects (Dudley et al. 2011, Chiang and Butte 2009, Campillos et al. 2008). These studies incorporate the rich information from expert curated biological knowledge databases, which represent the current understanding but may often be incomplete and inaccurate. In addition, the validation for these studies are typically based on internal data only. As a result, most of the identified drug repositioning opportunities have not been successfully translated into clinical practice.

Recent advances in genomic technology opened up opportunities for large scale association studies on drugs and biomarkers. Garrett et al. screened several hundred cancer cell lines under 130 drugs, identified some mutated genes that were associated with sensitivity to certain drugs (Garrett et al. 2012). The Connectivity Map (Lamb et al. 2006) offers an excellent data source on the effect of compounds on the gene expression level of cancer cell lines, and has been used by researchers for drug repositioning (Dudley et al. 2011, Zerbini et al. 2014). However, the data are from a few isolated cell lines *in vitro*, which may not reflect the true effect *in vivo*. Consequently, most studies typically focus on the gene signature changes rather than long-term clinical outcomes. Further, the effects of phenotypic information are often ignored in these studies (Spainhour and Qiu 2016, Hanahan and Weinberg 2011, Rubio-Perez et al. 2015).

The end goal for the drug repositioning research would be to inform the selection of personalized drug combinations given a patient's genomic and phenotypic data, completing the bench-to-bedside translation. In clinical settings, treatment selection is still based on one or two signatures. To extend to multiple targets and combination treatments, some network-based approaches were taken to infer combinatorial drug effects (Tang et al. 2013). Alternatively, gene expression-based methods were also considered - for instance, Pritchard et al. used a signature-based approach and identified cytotoxic chemotherapy combination mechanisms (Pritchard et al. 2013); Zhao et al. further incorporated drug efficacy and side effects to derive optimal combinations (Zhao et al. 2014). On the phenotypic side, some recent work by Bertsimas et al. built a large database of clinical trials and used machine learning/optimization to design combination chemotherapy regimens for cancer (Bertsimas et al. 2016). It is an important step towards personalized cancer therapy, although the nature of the aggregate data prevents it from fully capturing individual heterogeneity.

This study offers a data-driven approach to repurpose existing drugs by identifying novel drug-target relations. By integrating clinical and genomic data from thousands of patients at a large national cancer hospital with knowledge from biological processes, we are able to infer the interactions between drugs and targets from the binary coefficients of a non-linear regression analysis,

learned via mixed-integer optimization. Our model outputs a priority list of candidate targets for each drug to be further investigated. The inferred relations are validated against some of the known mechanisms of certain drugs.

Without randomized clinical trials, it is impossible to establish causal relationships from observational data only. We make a number of assumptions for our inferred drug and target interactions to be valid. We assumed a Bayesian Network model structure with hidden variables to be the underlying ground-truth causal model. The model is assumed to have enough capacity to represent the relationships (linear effects of the demographic and medical information, for example). We also assume that the data is sufficiently large for the inference. Under these assumptions, the mixed-integer optimization approach can then correctly recover with high precision the ground-truth drug-target relationships. We show this in a synthetic experiment where the ground-truth is known.

Because one cannot verify the validity of the assumptions given the observational nature of the data, the causal effects we inferred will still need to be confirmed by direct randomized experimentation. As a proxy, we test whether our assumed network model represents ground-truth causal model closer than simple ones by evaluating the generalization performance against simpler linear models in a hold-out test set and an external data set using the Cancer Genome Atlas.

The findings provide a natural pathway towards personalized, mechanism-guided cancer therapy. Quantifying the impact of each agent in the signaling network allows for more precise treatment selection that target the relevant pathways therapeutically, preventing the relapses often seen in targeted therapies. Given a patient with demographic, medical, and genomic information, the model allows practitioners to select combination therapies that holistically maximizes the long-term effectiveness by targeting the right processes while maintaining low level of off-target toxicity.

## 2. Data and Methods

### 2.1. Data

We retrospectively obtained the electronic health records (EHR) data for patients at the Dana-Farber/Brigham and Women’s Cancer Center (DFCI) from 2004-2014. There are

- $i = 1, \dots, n$  patients,
- $j = 1, \dots, m$  treatments  $T_j$ ,
- $k = 1, \dots, K$  gene mutations  $G_k$ ,
- $\ell = 1, \dots, L$  sets  $S_\ell$  that consists of genes (please see the significance in Section 2.2).

For each patient  $i$  we have the following information:

$$G_{ik} = \begin{cases} 1, & \text{if gene mutation } G_k \text{ is present in patient } i, \\ 0, & \text{otherwise,} \end{cases}$$

and

$$T_{ij} = \begin{cases} 1, & \text{if patient } i \text{ received treatment } T_j, \\ 0, & \text{otherwise.} \end{cases}$$

In addition,  $\mathbf{x}_i$  is the  $D$ -dimensional vector of phenotype covariates for patient  $i$ , including demographics, cancer diagnoses, comorbidities, prior treatments, resource utilization, and vital signs/laboratory tests results.  $y_i$  is the observed survival time in days for patient  $i$  from initiation of anti-cancer regimen, including chemotherapy, immunotherapy, and targeted therapy.

To be eligible for the study, patients must have initiated at least one anti-cancer regimen at the cancer center. Furthermore, patients are required to have measurements from *OncoPanel/OncoMap*, a sequencing platform that detects genetic mutations and other cancer-related DNA alterations.

We further obtained auxiliary data from curated biological and pharmacological databases. The sets  $S_\ell$ ,  $\ell = 1, \dots, L$  are obtained from Molecular Signatures Database, a curated database representing canonical pathways (Subramanian et al. 2005, Kanehisa and Goto 2000), which is widely used as a reference knowledge base for the interpretation and analysis of datasets generated from genome sequencing.

Missing values were imputed using unconditional mean; the results based on other imputation algorithms such as *knn-impute* (Troyanskaya et al. 2001) and *optimal-impute* (Bertsimas et al. 2017) are included in sensitivity analyses. We used regimens initiated from 2004-11 as the training set, and used regimens initiated from 2012-14 as the validation set. The institutional review boards of the associated institutions (anonymized here) approved this study.

## 2.2. Model

It is widely believed that mutations in tumor suppressor genes or oncogenes are linked to the development of cancer. Such genes are involved in critical signaling pathways that regulate cell cycles. When a mutation is present, the protein expression for that gene can be abnormal and adversely affect cell functions controlled by the pathway, subsequently affecting patient survival. In this section, we build the mathematical model of cancer treatments based on this biological mechanism, the structure of which are based on well-known literature in cancer including Hanahan and Weinberg (2011), Weinberg (2013), Sawyers (2004).

Targeted therapies, as an effective treatment of cancer, are known to interfere with the action of some proteins expressed by the mutated genes ( $G_k$ ) by inhibiting their functions. However, it is unknown whether a treatment  $T_j$  targets a specific mutation  $G_k$ . Correspondingly, our key decision variable is to infer from data:

$$w_{jk} = \begin{cases} 1, & \text{if treatment } T_j \text{ targets gene mutation } G_k, \\ 0, & \text{otherwise.} \end{cases} \quad (1)$$

We postulate that time of survival  $y_i$  of patient  $i$  is affected by the vector of phenotype covariates  $\mathbf{X}_i$ , and specifically decreases when there are abnormal gene expressions that are not targeted by appropriate therapies. In particular, groups of gene expressions  $S_\ell$  function together to affect survival. Mathematically we assume the following form (where we denote observed data  $y_i, \mathbf{x}_i$  with lower-case letters, but unobserved variables with capital letters  $Y_i, \mathbf{X}_i$ ):

$$Y_i = \exp(\beta_0 + \mathbf{X}_i^T \boldsymbol{\beta} - \sum_{\ell=1}^L r_\ell s_{i\ell}), \quad (2)$$

where  $\beta_0$  is the bias term,  $\boldsymbol{\beta}$  is a  $D$ -dimensional vector to be estimated that models the influence of the corresponding phenotype  $\mathbf{X}_i$ , the variable  $r_\ell$  to be estimated is the influence of having an abnormal set  $S_\ell$ , and the decision variable  $s_{i\ell}$  is defined as follows:

$$s_{i\ell} = \begin{cases} 1, & \text{if some gene expression for patient } i \text{ in the set } S_\ell \text{ is abnormal,} \\ 0, & \text{otherwise.} \end{cases} \quad (3)$$

**Table 1** Data and variable descriptions for the network model

| Data/Variable  | Definition   |
|----------------|--|
| $T_{ij}$       | Patient $i$ received treatment $T_j$                                     |
| $G_{ik}$       | Gene mutation $G_k$ is present in patient $i$                            |
| $\mathbf{x}_i$ | Phenotype covariates of patient $i$                                      |
| $S_\ell$       | Gene set $\ell$  |
| $y_i$          | Survival in days for patient $i$   |
| $w_{jk}$       | Treatment $T_j$ targets gene mutation $G_k$                              |
| $g_{ik}$       | Gene mutation $G_k$ is present in patient $i$ but not targeted           |
| $\beta$        | Linear effect of covariate $\mathbf{x}$                                  |
| $\beta_0$      | Bias term  |
| $s_{i\ell}$    | Whether some gene expression for patient $i$ in set $S_\ell$ is abnormal |
| $r_\ell$       | Effect of having an abnormal set $S_\ell$                                |

We obtain from Eq. (2) that

$$\log(Y_i) = \beta_0 + \mathbf{X}_i^T \beta - \sum_{\ell=1}^L r_\ell s_{i\ell}, \quad (4)$$

i.e., presence of an abnormal set  $S_\ell$  of gene expressions decreases life span by  $r_\ell$  log days.

In summary, therapies target gene expressions. A gene expression is abnormal if the corresponding mutation is present and a blocking therapy is not applied to the patient. If a gene expression is abnormal, then all sets  $S_\ell$  that contain it are also abnormal, and thus survival time is negatively affected from Eq. (4). Our objective is to infer the principal variable  $w_{jk}$ , defined in Eq. (1), the vector  $\beta$ , and the coefficients  $r_\ell$ . In the process of inferring the above principal variables, we also infer auxiliary variables  $s_{i\ell}$  defined in Eq. (3), gene expression variable

$$g_{ik} = \begin{cases} 1, & \text{if gene mutation } G_k \text{ is present in patient } i \text{ but not targeted,} \\ 0, & \text{otherwise;} \end{cases} \quad (5)$$

as well as the product between  $r_\ell$  and  $s_{i\ell}$ , denoted by:

$$v_{i\ell} = r_\ell s_{i\ell} = \begin{cases} r_\ell, & \text{if } s_{i\ell} = 1, \\ 0, & \text{otherwise.} \end{cases} \quad (6)$$

Figure 1 depicts the inference problem we are solving, with the data and variables summarized in Table 1.

Because of the logical relations among the variables, the model can be naturally formulated using Mixed Integer Optimization (MIO) (Bertsimas and Weismantel 2005). MIO is a particularly flexible



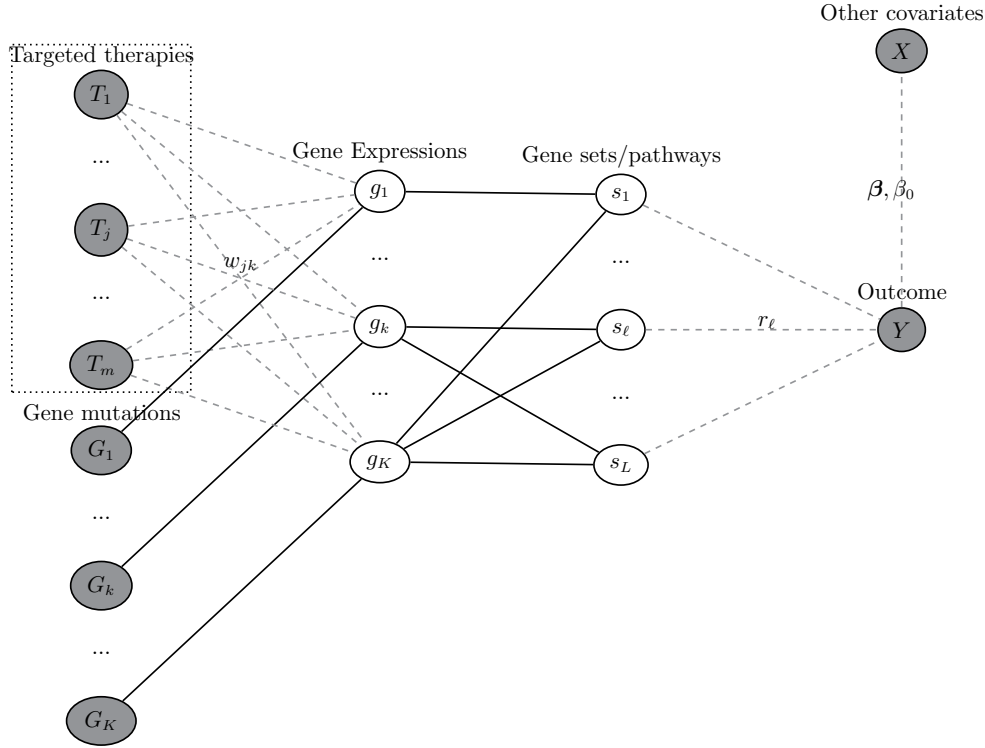


**Figure 1** Model network incorporating the treatments, gene mutations, gene expressions, signaling pathway gene sets, phenotype covariates, and the survival outcomes. The dashed edges  $w_{jk}$  and the coefficients  $r_\ell$  and  $\beta$  need to be determined by the mixed integer optimization problem. The solid edges and shaded variables are known and represent inputs to our model. The unshaded variables are derived.

tool for mathematical modeling, especially for incorporating logical constraints and relationships among variables and data. In recent years, advances in algorithms and computational hardware allowed a speedup of over several trillion times for solving MIO models, making even complex, large-scale problems tractable. We therefore selected it as our modeling technique.

The full MIO model formulation is as follows, with  $i \in [n]$  et al. as shorthand notation for the enumeration  $i \in 1, \dots, n$ , et al.:

$$\min_{\mathbf{w}, \mathbf{g}, \beta, \beta_0, \mathbf{s}, \mathbf{r}} \sum_{i=1}^n |\log(y_i) - (\beta_0 + \mathbf{x}_i^T \boldsymbol{\beta} - \sum_{\ell=1}^L v_{i\ell})| \quad (7a)$$

$$+ \lambda \sum_{j,k} w_{jk} + \gamma |\boldsymbol{\beta}|_1 \quad (7b)$$

$$\text{s.t. } g_{ik} \leq G_{ik}, \quad \forall i \in [n], k \in [K], \quad (7c)$$

$$\sum_{j=1}^m T_{ij} w_{jk} \leq (\sum_{j=1}^m T_{ij})(1 - g_{ik}), \quad \forall i \in [n], k \in [K], \quad (7d)$$

$$G_{ik} - \sum_{j=1}^m T_{ij} w_{jk} \leq g_{ik}, \quad \forall i \in [n], k \in [K], \quad (7e)$$

$$g_{ik} \leq s_{i\ell}, \quad \forall i \in [n], \ell \in [L], k \in S_\ell, \quad (7f)$$

$$\sum_{k \in S_\ell} g_{ik} \geq s_{i\ell}, \quad \forall i \in [n], \ell \in [L], \quad (7g)$$

$$v_{i\ell} \leq M s_{i\ell}, \quad \forall i \in [n], \ell \in [L], \quad (7h)$$

$$v_{i\ell} \leq r_\ell, \quad \forall i \in [n], \ell \in [L], \quad (7i)$$

$$v_{i\ell} \geq r_\ell - M(1 - s_{i\ell}), \quad \forall i \in [n], \ell \in [L], \quad (7j)$$

$$v_{i\ell} \geq 0, \quad \forall i \in [n], \ell \in [L], \quad (7k)$$

$$r_\ell \geq 0, \quad \forall \ell \in [L], \quad (7l)$$

$$s_{i\ell} \in \{0, 1\}, \quad \forall i \in [n], \ell \in [L], \quad (7m)$$

$$w_{jk} \in \{0, 1\}, \quad \forall j \in [m], k \in [K], \quad (7n)$$

$$g_{ik} \in \{0, 1\}, \quad \forall i \in [n], k \in [K], \quad (7o)$$

$$\beta \in \mathcal{R}^D, \beta_0 \in \mathcal{R}. \quad (7p)$$

The objective function Eq. (7b) finds parameters to achieve high goodness-of-fit on empirical data (first term), as well as giving preference to simpler and sparser models (second and third terms). The penalty  $\lambda$  encourages fewer drug-target interactions identified, and  $\gamma$  is the coefficient for standard lasso-type  $\ell_1$  regularization (Tibshirani 1996). The values are selected via cross validation, a procedure where an unseen dataset is used to evaluate the best parameter choice for out-of-sample performance.

The constraints describe the biological mechanism and logical relationships in our model. Eqs. (7c), (7d), and (7e) jointly impose the logical definition in Eq. (5). Specifically, from Eq. (7c) if  $G_{ik} = 0$  then  $g_{ik} = 0$ , i.e., if mutation  $G_k$  is not present in patient  $i$ , then gene expression  $g_k$  is normal for this patient. From Eq. (7d), if there is a therapy  $T_j$  that patient  $i$  received and  $T_j$  targets mutation  $G_k$ , then  $g_{ik} = 0$ . From Eq. (7e), if  $G_{ik} = 1$  and  $\sum_{j=1}^m T_{ij} w_{jk} = 0$ , i.e., mutation is present but no targeting therapy is given, then  $g_{ik} = 1$ .

Eqs. (7f) and (7g) jointly impose the logical defined in Eq. (3). From Eq. (7f), if for some  $k$  in  $S_\ell$  we have  $g_{ik} = 1$ , then  $s_{i\ell} = 1$ , i.e., if a gene expression  $g_k$  in patient  $i$  is abnormal, then all sets  $S_\ell$  containing  $g_k$  are abnormal. From Eq. (7g), if  $\sum_{k \in S_\ell} g_{ik} = 0$ , then  $s_{i\ell} = 0$ ; that is, if all of the gene expressions in  $S_\ell$  are normal, then the set  $S_\ell$  is normal.

Finally Eqs. (7h), (7i), and (7j) jointly define the nonlinear relationship between the  $s_\ell$  and the coefficients  $r_\ell$  as defined in Eq. (6).

The key output of the MIO (7) are the binary variables  $w_{jk}$  that represent our prediction of whether treatment  $T_j$  targets mutation  $G_k$ . We also produce confidence estimates for  $w_{jk}$  by using the bootstrap method via sampling the data with replacement (Efron 1979), solving the MIO (7) multiple times, and aggregating the results. To ensure the model generalizes well to different population, in addition to bootstrapping with random resampling, we also include subsamples based on some simple propensity model on the patient demographic information.

### 2.3. Evaluations

**2.3.1. Model Fit Comparisons** To validate that the MIO (7) model fits and generalizes better to real clinical outcomes than existing methods, we compare it against predictions made from linear models. We consider the following three models, each fitted on  $\log(y)$  to minimize the total sum of absolute error, to be consistent with the MIO objective for a fair comparison:

- LM1: with phenotype covariates alone;
- LM2: with phenotype covariates plus treatments and gene mutations;
- LM3: with phenotype covariates, treatments, gene mutations, and the interactions between treatments and gene mutations. The interactions terms measure the incremental effects from a given treatment when a patient has a specific mutation. It is a common method for estimating individual treatment effects (Imai et al. 2013).

Regularization is used when the variables are in high dimensions. Each model is cross-validated to select best regularization parameter choice. Similar to bootstrapping with special subpopulation, the cross-validation procedure also includes subpopulation in addition to random sampled population splits. The in-sample and out-of-sample performance measured as mean absolute error (MAE) of each model is reported.

**2.3.2. Inferred Therapy-Target Accuracy** The key model output is the inferred values for variable  $w_{jk}$  on whether therapy  $T_j$  targets mutation  $G_k$ . It is, however, unknown what the ground truth is. Therefore, evaluating the accuracy of our inferred therapy-target pairs is not feasible.

To gain a rough sense on the quality of  $w_{jk}$  predictions, we use the current biomedical knowledge on existing drugs as a proxy for the ground truth. To do so, we obtain data from the Drugbank

database that has current knowledge on drug data and target information (Law et al. 2013). The current understanding of therapy-target relations from this database is considered as ground truth, where our findings are evaluated against it. The accuracy, true positive, and false positive rates are reported. Note that since the current knowledge has likely not discovered some true relationships, the estimated true positive and false positive rates from our model are quite conservative.

**2.3.3. Further Validations** We further validate the model externally on an additional dataset from the Cancer Genome Atlas (TCGA). TCGA is a program launched by the National Cancer Institute (NCI) and National Human Genome Research Institute (NHGRI), with a goal to accelerate cancer research with comprehensive data on tumor samples. We extracted a similar set of genomic and clinical information from breast cancer, lung cancer, and skin cancer patients and ran the MIO (7) model to estimate the  $w_{jk}$ . The same set of model evaluations with model fit and inferred therapy-target accuracy were performed.

Finally, we perform an experiment on synthetically-generated data where the ground truth of the therapy-target relations variable  $w_{jk}$  is known. The goal is to validate that solving MIO (7) can recover the relationships assuming the model is an accurate description of the biological process. We first generate values for the principal variables  $w_{jk}$ ,  $\beta$ , and  $r_\ell$ ; next, we simulate the patient phenotype covariates  $\mathbf{x}_i$ , gene mutation  $G_{ik}$ , and treatments  $T_{ij}$ . Finally, we calculate the survival outcome  $y_i$  based on the model structure described in Section 2.2 with varying levels of additive noise. Because the ground truth for  $w_{jk}$  is known, we can evaluate the accuracy, true positive, and false positive rates of the inferred values.

The software used includes R (3.3.3), Julia (0.6.0), and Gurobi Optimizer (7.0).

### 3. Results

From the Dana Farber Cancer Institute (DFCI) data set, we obtained the genetic and clinical data of 3,118 eligible patients. Common cancer sites include breast, ovary, lung, and colon/rectum. In total, these patients initiated  $n = 6,928$  anti-cancer regimens. The median survival from the initiation of therapy is 550 days. Phenotype covariates (133 variables) include race, age, gender,

tumor site, stage, metastatic status, comorbidities, laboratory test results, and major medications, with age at treatment (correlation coefficient of  $-0.1790$ , same measures below), age at diagnosis ( $-0.1626$ ), and clinical stage IV ( $-0.1299$ ) most negatively correlated with survival. The most frequently mutated genes are TP53, PIK3CA, and MYC (Figure 2, top) among  $K = 176$  total measured gene mutations. The presence of most mutations are negatively correlated with the survival outcome, with TCF7L2 ( $-0.0615$ ), CDKN2B ( $-0.0606$ ), and PTEN ( $-0.0578$ ) being the most negatively correlated. Among all prescribed chemotherapy drugs, the most commonly ones include carboplatin, paclitaxel, and cisplatin. Targeted therapies are less frequently prescribed, but we included the following  $m = 10$  therapies that have sufficient observations: bevacizumab, trastuzumab, cetuximab, rituximab, ipilimumab, pertuzumab, pembrolizumab, panitumumab, erlotinib, and bortezomib. Among these, the use of trastuzumab ( $0.1351$ ) and rituximab ( $0.0811$ ) is most positively correlated with survival.

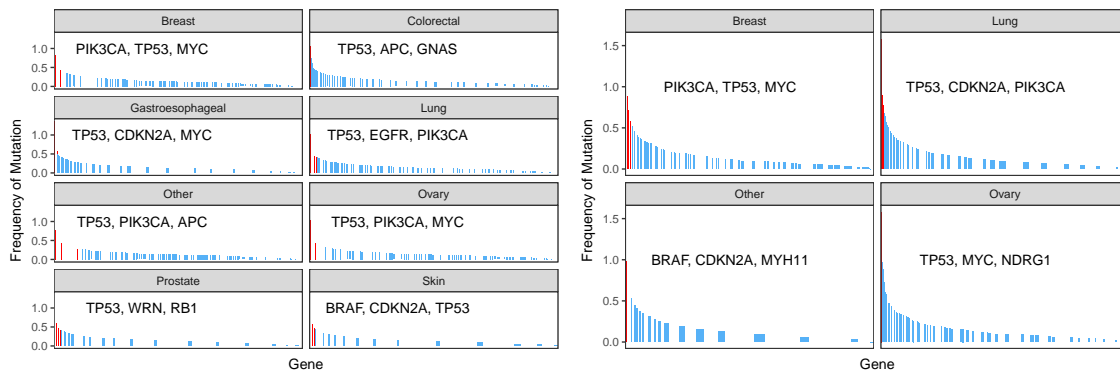


**Figure 2** Most frequently mutated genes among all observations, stratified by the tumor site for DFCI on the top and TCGA on the bottom. The top three mutations for each site is highlighted in red and the gene is labeled.

From the Cancer Genome Atlas data set, we obtained the genetic and clinical data of 1,098 eligible patients from the following projects: breast invasive carcinoma, ovarian serous cystadenocarcinoma, lung squamous cell carcinoma, lung adenocarcinoma, and skin cutaneous melanoma. In total, these patients initiated 6,929 regimens. The median survival from the initiation of therapy is 529 days. Phenotype covariates used include race, gender, tumor site, age at diagnosis, history of neoadjuvant treatment, history of radiation therapy, and some breast cancer specific

ones (menopause status, estrogen receptor status, etc.). The most frequently mutated genes are TP53, PIK3CA, MYC, NDRG1, EXT1, RAD21 (Figure 2, bottom) out of a total of 299 common gene mutations under consideration. Among all prescribed chemotherapy drugs, the most commonly ones include paclitaxel, carboplatin, cyclophosphamide, doxorubicin, docetaxel, cisplatin, and tamoxifen. Targeted therapies are less frequently prescribed, but we included the following that have sufficient observations: bevacizumab, trastuzumab, erlotinib, ipilimumab, vemurafenib, gefitinib, denosumab, aldesleukin, and dabrafenib.

### 3.1. Model Fit Comparisons

Comparing the proposed mixed integer optimization (MIO) (7) model against linear regression models, we achieved better model generalization performance, as reflected in the lower mean absolute error (MAE) (Table 2) for both DFCI and TCGA data. Adding to LM1 (phenotypic information only) genomic data and treatment data as additional terms (LM2 and LM3) typically does not improve the generalization performance, even with appropriate level of regularization. In contrast, because the MIO (7) model directly optimizes the sum of absolute error while maintaining sparsity, it improves upon any linear models significantly under MAE as the goodness-of-fit metric.

Between the two data sources, the DFCI one has very rich phenotype data that are likely to be predictive of the survival outcomes (Bertsimas et al. 2018), and therefore was able to achieve lower MAE both in sample and out of sample. The TCGA data has abundant information on genomic data; however, even with regularization there is still some discrepancy between the in-sample and out-of-sample performance metrics. We attribute this discrepancy to the inherent high-dimensional nature of the data.

### 3.2. Inferred Therapy-Target Accuracy

The model outputs therapy-target pairs from solving MIO (7) with the DFCI data. Because the interactions are probabilities averaged from bootstrapped samples, at any chosen probability threshold cutoff, we can obtain a set of inferred interactions. We choose the threshold  $\delta$  such that if the calculated confidence probability is greater than  $\delta$  for a particular therapy-target combination,

**Table 2** Model performance comparisons for DFCI and TCGA data. The in-sample and out-of-sample mean absolute errors are reported for each of the four models being compared.

| Data  | Model | In-Sample MAE | Out-of-Sample MAE |
|-------|-------|---------------|-------------------|
|       | LM1   | 0.65          | 0.73              |
|       | LM2   | 0.64          | 0.71              |
| DFCI  | LM3   | 0.62          | 0.71              |
|       | MIO   | 0.66          | 0.69              |
| ----- |       |               |                   |
|       | LM1   | 0.89          | 0.92              |
|       | LM2   | 0.77          | 0.97              |
| TCGA  | LM3   | 0.73          | 0.99              |
|       | MIO   | 0.88          | 0.91              |

**Table 3** Confusion table for estimated  $w_{jk}$  based on DFCI and TCGA data, comparing predicted therapy-target relationships against ones known from literature.

| DFCI        | Actual 0 | Actual 1 |
|-------------|----------|----------|
| Predicted 0 | 1684     | 3        |
| Predicted 1 | 70       | 3        |
| =====       |          |          |
| TCGA        | Actual 0 | Actual 1 |
| Predicted 0 | 3524     | 11       |
| Predicted 1 | 49       | 4        |
| =====       |          |          |

then we include this combination in the output we report, in a way to limit the number of distinct therapy-target combinations. When validating against known relationships, we aim at keeping around 60 predicted pairs, which correspond to a threshold of 0.34. The prediction achieved an accuracy of 95.8%, a true positive rate of 50.0%, and a false positive rate of 4.0% (Table 3, top section).

**Table 4** Potential drug-target relationships identified by model, ordered by descending probabilities. The relationships known in literature are highlighted.

| Drug          | Target | Probability | Drug          | Target | Probability |
|---------------|--------|-------------|---------------|--------|-------------|
| pembrolizumab | TP53   | 0.92        | panitumumab   | BCL2   | 0.48        |
| trastuzumab   | AKT2   | 0.74        | cetuximab     | PIK3CA | 0.48        |
| pertuzumab    | PTK2   | 0.74        | panitumumab   | FGFR1  | 0.46        |
| rituximab     | SRC    | 0.74        | pembrolizumab | MET    | 0.46        |
| pembrolizumab | CDK4   | 0.70        | cetuximab     | MTOR   | 0.46        |
| bevacizumab   | MAPK1  | 0.70        | ipilimumab    | FLT4   | 0.44        |
| pembrolizumab | MAPK1  | 0.70        | cetuximab     | PTK2   | 0.44        |
| panitumumab   | SRC    | 0.70        | cetuximab     | BRAF   | 0.42        |
| panitumumab   | IGF1R  | 0.68        | panitumumab   | JAK2   | 0.42        |
| rituximab     | PIK3CA | 0.68        | panitumumab   | NTRK3  | 0.42        |
| erlotinib     | TP53   | 0.68        | ipilimumab    | RAF1   | 0.42        |
| pembrolizumab | MTOR   | 0.66        | rituximab     | AKT1   | 0.40        |
| rituximab     | TP53   | 0.66        | bevacizumab   | AKT3   | 0.40        |
| cetuximab     | AKT3   | 0.64        | pertuzumab    | ERBB2  | 0.40        |
| panitumumab   | PTK2   | 0.64        | cetuximab     | IGF1R  | 0.40        |
| pertuzumab    | MAP3K1 | 0.62        | erlotinib     | MET    | 0.40        |
| bevacizumab   | PIK3CA | 0.62        | pertuzumab    | PRKDC  | 0.40        |
| panitumumab   | TP53   | 0.62        | trastuzumab   | SRC    | 0.40        |
| trastuzumab   | AKT3   | 0.60        | pertuzumab    | SRC    | 0.40        |
| trastuzumab   | RAF1   | 0.60        | trastuzumab   | SYK    | 0.40        |
| pembrolizumab | EGFR   | 0.58        | pertuzumab    | SYK    | 0.40        |
| rituximab     | PTEN   | 0.58        | trastuzumab   | AKT1   | 0.38        |
| erlotinib     | EGFR   | 0.56        | pertuzumab    | AKT1   | 0.38        |
| pembrolizumab | FGFR3  | 0.56        | ipilimumab    | EGFR   | 0.38        |
| bevacizumab   | AKT1   | 0.54        | bevacizumab   | IGF1R  | 0.38        |
| bevacizumab   | BRAF   | 0.54        | pertuzumab    | TP53   | 0.38        |
| trastuzumab   | MAPK1  | 0.54        | cetuximab     | AKT2   | 0.36        |
| bevacizumab   | SRC    | 0.54        | panitumumab   | AURKA  | 0.36        |
| bevacizumab   | TP53   | 0.54        | panitumumab   | BCL2L1 | 0.36        |
| panitumumab   | MAPK1  | 0.52        | panitumumab   | PTEN   | 0.36        |
| pertuzumab    | PIK3CA | 0.52        | pertuzumab    | PTPN11 | 0.36        |
| cetuximab     | RAF1   | 0.52        | cetuximab     | EGFR   | 0.34        |
| cetuximab     | SRC    | 0.52        | ipilimumab    | MAP3K1 | 0.34        |
| pembrolizumab | BRAF   | 0.50        | trastuzumab   | PIK3CA | 0.34        |
| pembrolizumab | JAK2   | 0.50        | bevacizumab   | PRKDC  | 0.34        |

Sorting the predicted probabilities of therapy-target interactions gives a list to be further investigated in experiments (Table 4). We correctly recovered the well-known therapy-target pairs including erlotinib on EGFR, pertuzumab on ERBB2, and cetuximab on EGFR at this threshold. At a lower threshold of 0.20, we also discover temsirolimus on MTOR and panitumumab on EGFR. The relationship trastuzumab on ERBB2 was not identified, likely because data do not suggest pronounced incremental treatment effects from trastuzumab on patients with ERBB2 mutation.

We conducted similar analysis for the TCGA data. To obtain about 60 therapy-target pairs, we selected the threshold of 0.38. The prediction achieved an accuracy of 98.3%, a true positive rate of 26.7%, and a false positive rate of 1.4% (Table 3, bottom section). The prediction provides the list of most promising therapy-target to be further investigated in experiments (Table 5). We correctly



**Table 5** Potential drug-target relationships identified by model, ordered by descending probabilities. The

relationships known in literature are highlighted.

| Drug          | Target  | Probability | Drug          | Target  | Probability |
|---------------|---------|-------------|---------------|---------|-------------|
| dabrafenib    | BRAF    | 0.98        | bevacizumab   | PIK3CA  | 0.64        |
| denosumab     | IKBKB   | 0.98        | pembrolizumab | LCK     | 0.62        |
| vemurafenib   | BRAF    | 0.90        | vemurafenib   | MET     | 0.62        |
| ipilimumab    | CACNA1D | 0.86        | trastuzumab   | TP53    | 0.62        |
| trastuzumab   | MAPK1   | 0.86        | pembrolizumab | GRIN2A  | 0.60        |
| cetuximab     | PRKACA  | 0.86        | trastuzumab   | IKBKB   | 0.58        |
| dabrafenib    | FGFR2   | 0.84        | lapatinib     | MAP2K2  | 0.58        |
| denosumab     | PIK3CA  | 0.84        | bevacizumab   | IKBKB   | 0.56        |
| cetuximab     | TP53    | 0.84        | pembrolizumab | MLH1    | 0.56        |
| erlotinib     | NTRK1   | 0.82        | lapatinib     | PIK3CA  | 0.56        |
| cetuximab     | PIK3CA  | 0.80        | pembrolizumab | PMS2    | 0.56        |
| ipilimumab    | AKT2    | 0.78        | erlotinib     | TSHR    | 0.56        |
| pembrolizumab | BRAF    | 0.78        | gefitinib     | EGFR    | 0.54        |
| gefitinib     | TP53    | 0.76        | lapatinib     | ERBB2   | 0.54        |
| vemurafenib   | AKT2    | 0.74        | trastuzumab   | JAK1    | 0.54        |
| dabrafenib    | BCR     | 0.74        | erlotinib     | MDM2    | 0.54        |
| cetuximab     | MET     | 0.74        | erlotinib     | PDGFRA  | 0.54        |
| dabrafenib    | NFKB2   | 0.74        | aldesleukin   | AKT2    | 0.52        |
| erlotinib     | TP53    | 0.74        | aldesleukin   | BRAF    | 0.52        |
| cetuximab     | BRAF    | 0.72        | bevacizumab   | CACNA1D | 0.52        |
| dabrafenib    | PTEN    | 0.72        | dabrafenib    | KDR     | 0.52        |
| ipilimumab    | TP53    | 0.72        | cetuximab     | MAP2K4  | 0.52        |
| dabrafenib    | PDGFRA  | 0.70        | lapatinib     | TP53    | 0.52        |
| vemurafenib   | PTEN    | 0.70        | lapatinib     | BCR     | 0.50        |
| trastuzumab   | PIK3CA  | 0.68        | erlotinib     | IKBKB   | 0.50        |
| denosumab     | FGFR1   | 0.66        | lapatinib     | MALT1   | 0.50        |
| bevacizumab   | GRIN2A  | 0.66        | erlotinib     | PIK3CA  | 0.50        |
| cetuximab     | JAK1    | 0.66        | bevacizumab   | POLE    | 0.50        |
| ipilimumab    | ATP1A1  | 0.64        | trastuzumab   | PRKACA  | 0.50        |
| ipilimumab    | BRAF    | 0.64        | lapatinib     | ATM     | 0.48        |

recovered the well-known relationships of dabrafenib on BRAF, vemurafenib on BRAF, gefitinib on EGFR, and lapatinib on ERBB2.

While interpreting the results, note that again since the known pairs used to validate our model against are not exactly the ground truth, as many pairs remain to be discovered, the reported model performance metrics of true positive and false positive rates may be overly conservative.

### 3.3. Synthetic Data Validation

In the validation studies with synthetic data, we confirmed that when the causal assumptions are met, the inferred values of  $w_{jk}$  are accurate. We ran the MIO (7) to assess the quality of recovery of  $w_{jk}$  based on synthetically generated data where the underlying parameters are known and the data follow the model structure. Figure 3 presents the model performance at varying levels of noise: the accuracy, true positive, and false positive rates are plotted against noise. At low levels of noise,

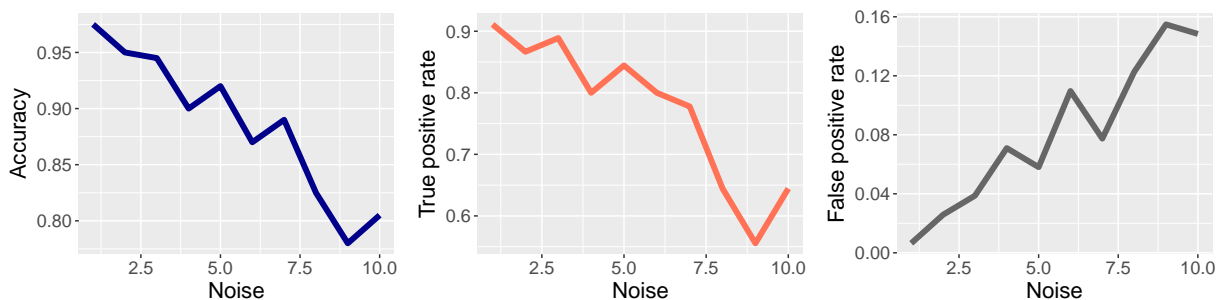


**Figure 3** Model performance on synthetic data for recovering the therapy-target relationship  $w_{jk}$ . The accuracy, true positive, and false positive rates against noise levels are presented.

the model achieves almost perfect recovery of  $w_{jk}$ ; as noise increases, the performance generally drops, but still remains reasonably high given the noise level.

#### 4. Discussion

To our knowledge, this is the first study to leverage rich genomic and clinical information from observational *in vivo* data to inform drug discovery. It uses modern mathematical modeling tools to integrate data and biological knowledge base to identify the most likely therapy-target interactions. The network-based, MIO model is able to capture the non-linear interaction between therapies and targets. Compared to black-box machine learning models, it outputs interpretable chemical and biological processes while still allowing for the flexibility to represent the complex interactions across the patient inputs.

This novel approach to drug discovery has the following advantages: 1) it is based on large scale real-world evidence to infer potential biochemical mechanisms, overcoming the limitation of many *in vitro* experiments; 2) it incorporates the state-of-the-art understanding of cancer molecular biology and signaling pathways organically into a data-driven method; 3) it models patient heterogeneity explicitly outside genomic information, controlling for and capturing the rich information from patients' electronic medical records. As a result, the output of potential therapy-target interactions from this model was able to achieve high accuracy in external validation compared to other approaches.

The study has the following limitations: it is based on observational data, which unavoidably contain confounding factors. As a result, the learned relationships cannot be proven causal unless

the assumptions we made hold true. The set of gene mutations measured is relatively small (296 measured mutations) in the DFCI dataset; in particular, this dataset did not have information on immune cells, therefore restricting our inference on the potential targets for immunotherapies. In addition, the available human knowledge of gene sets is not complete. For future work, drug dosing information could be incorporated. As some of the target relationships are validated against findings in previous literature in this study, further validation should be conducted in prospective *in vitro* experiments, animal models, and clinical trials.

Extensions to the model are straight-forward. Because the MIO has a very flexible structure, it allows researchers to readily incorporate novel biological discoveries and updated data. In closer collaboration with cancer biologists, geneticists, and pharmacologists, we can further fine-tune the network model to reflect more comprehensive and new knowledge in the targeted therapy mechanism of action. The scalability of the model encourages further computational discoveries using data from other institutions and potentially data consortium from multiple institutions. As the data availability and quality improves, we believe the model will recommend new targets with even higher confidence and accuracy.

Matching patients to the right set of therapies, especially when the genetic signatures and clinical presentations are complex, is the ultimate goal for personalized cancer therapy. In this work, we present a general method with validated findings on novel therapy-target interactions, which provide a firm foundation for an evidence-based design of targeted treatment recommendations. Looking ahead, this approach will present not only significant opportunities for discoveries and breakthroughs in cancer medicine, but also higher quality, more individualized care for patients.

## References

- Bertsimas D, Dunn J, Pawlowski C, Silberholz J, Weinstein A, Zhuo YD, Chen E, Elfiky AA (2018) Applied informatics decision support tool for mortality predictions in patients with cancer. *JCO Clinical Cancer Informatics* 2(2):1–11, URL <http://dx.doi.org/10.1200/CCI.18.00003>.
- Bertsimas D, O’Hair A, Relyea S, Silberholz J (2016) An analytics approach to designing combination chemotherapy regimens for cancer. *Management Science* 62(5):1511–1531.
- Bertsimas D, Pawlowski C, Zhuo YD (2017) From predictive methods to missing data imputation: An optimization approach. *The Journal of Machine Learning Research* 18(1):7133–7171.
- Bertsimas D, Weismantel R (2005) *Optimization over integers* (Dynamic Ideas Belmont).
- Campillos M, Kuhn M, Gavin AC, Jensen LJ, Bork P (2008) Drug target identification using side-effect similarity. *Science* 321(5886):263–266.
- Chen B, Butte A (2016) Leveraging big data to transform target selection and drug discovery. *Clinical Pharmacology & Therapeutics* 99(3):285–297.
- Chiang AP, Butte AJ (2009) Systematic evaluation of drug–disease relationships to identify leads for novel drug uses. *Clinical Pharmacology & Therapeutics* 86(5):507–510.
- DiMasi JA, Grabowski HG, Hansen RW (2016) Innovation in the pharmaceutical industry: new estimates of r&d costs. *Journal of health economics* 47:20–33.
- Druker BJ (2004) Imatinib as a paradigm of targeted therapies. *Advances in cancer research* 91:1–30.
- Dudley JT, Deshpande T, Butte AJ (2011) Exploiting drug–disease relationships for computational drug repositioning. *Briefings in bioinformatics* 12(4):303–311.
- Efron B (1979) Bootstrap methods: another look at the jackknife. *The annals of Statistics* 1–26.
- Garnett MJ, Edelman EJ, Heidorn SJ, Greenman CD, Dastur A, Lau KW, Greninger P, Thompson IR, Luo X, Soares J, et al. (2012) Systematic identification of genomic markers of drug sensitivity in cancer cells. *Nature* 483(7391):570.
- Hanahan D, Weinberg RA (2011) Hallmarks of cancer: the next generation. *cell* 144(5):646–674.
- Imai K, Ratkovic M, et al. (2013) Estimating treatment effect heterogeneity in randomized program evaluation. *The Annals of Applied Statistics* 7(1):443–470.

- Kanehisa M, Goto S (2000) Kegg: kyoto encyclopedia of genes and genomes. *Nucleic acids research* 28(1):27–30.
- Kesselheim AS, Treasure CL, Joffe S (2017) Biomarker-defined subsets of common diseases: policy and economic implications of orphan drug act coverage. *PLoS medicine* 14(1):e1002190.
- Lamb J, Crawford ED, Peck D, Modell JW, Blat IC, Wrobel MJ, Lerner J, Brunet JP, Subramanian A, Ross KN, et al. (2006) The connectivity map: using gene-expression signatures to connect small molecules, genes, and disease. *science* 313(5795):1929–1935.
- Law V, Knox C, Djoumbou Y, Jewison T, Guo AC, Liu Y, Maciejewski A, Arndt D, Wilson M, Neveu V, et al. (2013) Drugbank 4.0: shedding new light on drug metabolism. *Nucleic acids research* 42(D1):D1091–D1097.
- Li J, Lu Z (2012) A new method for computational drug repositioning using drug pairwise similarity. *Bioinformatics and Biomedicine (BIBM), 2012 IEEE International Conference On*, 1–4 (IEEE).
- Li J, Zheng S, Chen B, Butte AJ, Swamidass SJ, Lu Z (2015) A survey of current trends in computational drug repositioning. *Briefings in bioinformatics* 17(1):2–12.
- Li YY, Jones SJ (2012) Drug repositioning for personalized medicine. *Genome medicine* 4(3):27.
- Mestres J, Gregori-Puigjané E, Valverde S, Solé RV (2009) The topology of drug–target interaction networks: implicit dependence on drug properties and target families. *Molecular BioSystems* 5(9):1051–1057.
- Novartis (2017) Gleevec - prescribing information. URL [https://www.accessdata.fda.gov/drugsatfda\\_docs/label/2006/021588s0091b1.pdf](https://www.accessdata.fda.gov/drugsatfda_docs/label/2006/021588s0091b1.pdf).
- Paul SM, Mytelka DS, Dunwiddie CT, Persinger CC, Munos BH, Lindborg SR, Schacht AL (2010) How to improve r&d productivity: the pharmaceutical industry’s grand challenge. *Nature reviews Drug discovery* 9(3):203–214.
- Pritchard JR, Bruno PM, Gilbert LA, Capron KL, Lauffenburger DA, Hemann MT (2013) Defining principles of combination drug mechanisms of action. *Proceedings of the National Academy of Sciences* 110(2):E170–E179.

- Rubio-Perez C, Tamborero D, Schroeder MP, Antolín AA, Deu-Pons J, Perez-Llamas C, Mestres J, Gonzalez-Perez A, Lopez-Bigas N (2015) In silico prescription of anticancer drugs to cohorts of 28 tumor types reveals targeting opportunities. *Cancer cell* 27(3):382–396.
- Sawyers C (2004) Targeted cancer therapy. *Nature* 432(7015):294.
- Shaw AT, Yasothan U, Kirkpatrick P (2011) Crizotinib. *Nature Reviews Drug Discovery* 10(12):897–898.
- Spainhour JCG, Qiu P (2016) Identification of gene-drug interactions that impact patient survival in tcga. *BMC bioinformatics* 17(1):409.
- Subramanian A, Tamayo P, Mootha VK, Mukherjee S, Ebert BL, Gillette MA, Paulovich A, Pomeroy SL, Golub TR, Lander ES, et al. (2005) Gene set enrichment analysis: a knowledge-based approach for interpreting genome-wide expression profiles. *Proceedings of the National Academy of Sciences* 102(43):15545–15550.
- Tang J, Karhinen L, Xu T, Szwajda A, Yadav B, Wennerberg K, Aittokallio T (2013) Target inhibition networks: predicting selective combinations of druggable targets to block cancer survival pathways. *PLoS computational biology* 9(9):e1003226.
- Tibshirani R (1996) Regression shrinkage and selection via the lasso. *Journal of the Royal Statistical Society. Series B (Methodological)* 267–288.
- Troyanskaya O, Cantor M, Sherlock G, Brown P, Hastie T, Tibshirani R, Botstein D, Altman RB (2001) Missing value estimation methods for dna microarrays. *Bioinformatics* 17(6):520–525.
- US Food and Drug Administration (2016) Drug innovation - novel drugs summary 2016. URL <https://www.fda.gov/Drugs/DevelopmentApprovalProcess/DrugInnovation/ucm534863.htm>.
- Weinberg R (2013) *The biology of cancer* (Garland science).
- Zerbini LF, Bhasin MK, de Vasconcellos JF, Paccetz JD, Gu X, Kung AL, Libermann TA (2014) Computational repositioning and preclinical validation of pentamidine for renal cell cancer. *Molecular cancer therapeutics* 13(7):1929–1941.
- Zhao B, Hemann MT, Lauffenburger DA (2014) Intratumor heterogeneity alters most effective drugs in designed combinations. *Proceedings of the National Academy of Sciences* 111(29):10773–10778.